Time-dependent two-dimensional detonation: The interaction of edge rarefactions with finite length reaction zones

by

John B. Bdzil † and D. Scott Stewart ‡

† Los Alamos National Laboratory

‡ University of Illinois at Urbana-Champaign

Abstract

A theory of time-dependent two-dimensional detonation is developed for an explosive with a finite thickness reaction zone. A representative initial-boundary value problem is treated that illustrates how the planar shock of an initially one-dimensional detonation becomes nonplanar in response to the action of an edge rarefaction that is generated at the explosive's lateral surface. The solution of this time-dependent problem has a wave-hierarchy structure that at late times includes a weakly two-dimensional hyperbolic region and a fully two-dimensional parabolic region. The wave head of the rarefaction is carried by the hyperbolic region. We show that the shock locus is analytic at the wave head. The dynamics of the final approach to two-dimensional steady-state detonation is controlled by Burgers equation for the shock locus. We also present some results concerning the stability of the solutions to our problem.

1. Introduction

In this paper we present the first extension of the theory of steady, two-dimensional detonation waves [1,2], to include time dependent effects. We consider how an edge rarefaction, caused by a change in the confinement of the detonation, interacts with a finite thickness reaction zone to produce a nonplanar detonation. Specifically we describe the transients that carry an

initially one-dimensional detonation into a steady-state two-dimensional unsupported detonation. The following initial-boundary value problem is solved. Prior to time zero, an unsupported steady plane Zeldovich-von Neumann-Doering (ZND) detonation wave is propagating in an infinitely wide explosive. At time zero the detonation encounters a corner: an interface parallel to the original direction of propagation, with vacuum on the right and explosive on the left. The flow divergence produced by the expansion of the explosive products into the vacuum causes the leading shock to curve. After a sufficiently long time, the wave assumes an asymptotically steady profile.

The theory of the propagation of steady multidimensional detonation in a finite-width explosive or rate stick [1] (a pipe filled with explosive used in many standard explosive tests) is an asymptotic theory in which the reaction-zone thickness is assumed to be thin in comparison to a relevant flow dimension (the diameter of the explosive). The steady wave consists of a curved leading shock followed by the reaction zone. The leading-order properties of the detonation are determined by first solving an ordinary differential equation for the shock locus, subject to the condition that the shock slope is specified at the explosive/inert interface. Once the shock locus is found, the gas dynamic state in the reaction zone behind the shock is determined.

In our first attempt to generalize this steady result to include time dependence, we found that a description on a sufficiently slow time scale (compared to the $O(1)$ time scale for the reaction to occur), yields an unsteady theory which is a straightforward extension of the steady theory. The ordinary differential equation for the shock locus of the steady theory is replaced by a *parabolic* partial differential equation (PDE) in the slow time and a long distance along the shock. For one form of the reaction-rate law, this PDE is Burgers equation. The steady solution of this PDE is the steady multidimensional detonation solution described above.

The following question then arises: Given that the final approach to the steady state is controlled by a parabolic PDE, how does this equation arise from a hyperbolic system? If, in fact, an equation of parabolic type governs the important dynamics of stable detonation waves, then it is imperative that we show how such an equation arises naturally from the solution of a physically reasonable initial-boundary value problem in which the hyperbolic character of the problem is not compromised in any fundamental way. Our objective in this paper is to demonstrate how this transition in equation type occurs, and show that at late times the controlling shock dynamics is governed by a parabolic problem.

The plan of the article is as follows. In Section 2. we present the form of the reactive Euler equations appropriate for the model explosive that we analyze. Our model explosive has the property that only a small fraction,

δ^2, of the heat release is resolved in time. In Section 3. we analyze the dynamics of one-dimensional disturbances to plane unsupported steady detonation waves. We explicitly show which time scale is important in the absence of transverse disturbances. Sections 4. and 5. contain the principal results of this paper. In Section 4. we discuss the very long-time dynamics of the multidimensional detonation and derive the parabolic equation that describes its shock dynamics. We exhibit the temporal and spatial scales that are relevant for that description. In Section 5. we discuss the physical deficiences of the solution presented in Section 4. Namely, we point out that the infinite region of influence of the parabolic problem is not compatible with the finite communication times imposed by the underlying hyperbolic character of the flow. We then show that the deficiencies of the solution of Section 4. are resolved by noting the existence of a purely hyperbolic region, of small amplitude, that propagates ahead of the parabolic region. This hyperbolic region has a discrete wave head that propagates at a finite velocity and thus satisfies the physical boundary condition placed on the hyperbolic problem.

Figure 1 contains a summary of the results of Sections 4. and 5. for the small resolved heat-release explosive ($\delta \ll 1$) presented in Section 2. Of the three time scales indicated, we only consider $t \sim O(\delta^{-1})$ and $t \sim O(\delta^{-2})$ in this paper. On these two scales the flow is divided into three parts; the one-dimensional region (1-D), the hyperbolic or wave head region

(H), and the parabolic region (P). For $t \sim O(\delta^{-1})$ only the 1-D and hyperbolic regions are present. When $t \sim O(\delta^{-2})$ the hyperbolic equations govern only the near wave head flow, with most of the flow being controlled by the parabolic description.

Finally in Section 6. we discuss the results of our calculations. We elucidate the physically important aspects of the parabolic solution of the original initial-boundary value problem and also suggest possible future extensions and directions for this type of work.

2. Formulation and discussion of the model

In this section we give the formulation of our problem and discuss the motivation for the model that we use to describe the explosive equation of state (EOS).

We assume that the explosive is an Euler fluid. As such it is entirely modeled by specifying the form of the EOS and the rate law for heat release. In particular, the specific internal energy, E, is given by

$$\begin{aligned} &\textit{ahead of the shock}: \; E_0 = (\gamma - 1)^{-1} P_0 / \rho_0 \\ &\textit{behind the shock}: \; E = (\gamma - 1)^{-1} P/\rho - q\,[1 - \delta^2 (1 - \lambda)] \; . \end{aligned} \tag{2.1}$$

In the above, P, ρ and λ are the dependent variables pressure, density and the progress variable of a simple forward exothermic reaction. The parameters γ and q are respectively the polytropic exponent and the specific

heat of reaction of the explosive. While this EOS is quite similar to a standard EOS for a polytropic explosive used in [1], the model requires some further explanation.

When the parameter $\delta = 1$, the internal energy behind the leading shock is given by

$$E = (\gamma - 1)^{-1} P/\rho - q\lambda \ , \tag{2.2}$$

which is the polytropic EOS for an explosive with a fully resolved reaction zone. When the parameter $\delta = 0$, the EOS behind the leading shock is given by

$$E = (\gamma - 1)^{-1} P/\rho - q \ , \tag{2.3}$$

which is the polytropic EOS for an explosive for which all the energy release occurs instantaneously within the shock. In this limit the unsupported detonation is a Chapman-Jouguet (CJ) detonation.

In this paper we will be concerned with the case

$$\delta << 1 \ . \tag{2.4}$$

The heat released instantaneously in the shock is $q(1 - \delta^2)$. The remainder of the heat, $\delta^2 q$, is released by a reaction with a finite rate, where the progress of the temporally resolved heat release is measured by λ. At the leading shock $\lambda = 0$ and at the end of the reaction zone $\lambda = 1$. The assumption of an unresolved reaction zone within the leading shock can be justified if one assumes that there are actually two sequential reactions that release heat, the first being very rapid compared to the latter. We only

consider the case for which this first reaction layer is infinitesimally thin.

An important motivation for selecting this model is based on a property of real explosives. As one travels through the reaction zone in an unsupported ZND detonation, a disproportionately large pressure drop is associated with the last amount of heat release. This is most easily illustrated by formulas for a 1-D ZND wave as given in Fickett and Davis [3]. For example, the pressure in the reaction zone for a steady 1-D unsupported detonation with a polytropic EOS and fully resolved chemistry (i.e., $\delta = 1$), is given by

$$P = P_{CJ} \left(1 + \sqrt{1 - \lambda}\right) . \tag{2.5}$$

Near the shock, where $\lambda = 0$, the pressure is approximately

$$P = P_{CJ} \left(2 - \lambda/2\right) , \tag{2.6}$$

so that a 10% change in λ leads to a 2.5% pressure drop. However near the end of the reaction zone, where $\lambda \lesssim 1$, the pressure changes with the square root of changes in λ. According to (2.5), a 10% change in λ near $\lambda = 1$ leads to a 32% change in the pressure. Thus our model, which has a small amount of resolved heat release, reflects the important property that near the end of the reaction zone an $O(\delta^2)$ heat release is associated with a much larger $O(\delta)$ pressure drop.

There is another motivation for choosing this model. In order to have a cleanly defined edge-rarefaction initial-value problem, the 1-D detonation should be stable to local 2-D disturbances. Erpenbeck [4] has shown that

for the case of a fully resolved reaction zone with a state-independent rate, the 1-D detonation wave is unstable to local 2-D disturbances for a wide range of cases. However, Erpenbeck also showed that when the heat release of the detonation is smaller than the internal energy ahead of the shock (i.e., the weak shock limit), or when the detonation is strongly overdriven (i.e., when the heat release of the detonation is small compared to the energy input to the flow by the supporting piston), that the detonation *is* stable to local 2-D disturbances. In both instances, stability is found when the resolved detonation energy release is small compared to other energy terms in the system. For our model, namely that the unresolved heat release in the leading shock is much greater than that in the following flow, i.e.

$$\delta^2 / (1 - \delta^2) \ll 1 \ , \tag{2.7}$$

we might also expect to find that the 1-D steady detonation is stable to transverse disturbances. However we are obligated to show this. In Section 5. we prove stability.

We now give the formulation of the problem. The detonation wave is assumed initially to be a plane, steady unsupported detonation traveling at the CJ velocity D_{CJ}. The coordinate z^l measures distance in a stationary lab frame (l) in the direction of initial propagation, where $z^l = D_{CJ}\, t$ is the instantaneous position of the undisturbed shock and t is time. The disturbed shock locus is at $z^l = \psi(r,t) + D_{CJ}\, t$, where $\psi(r,t)$ measures the distance from the undisturbed 1-D shock locus. The coordinate r is

perpendicular to z^l and measures distance along the undisturbed shock. In our analysis we will use the basic independent variables

$$z\,,\,r \text{ and } t \quad , \tag{2.8}$$

where $z \equiv z^l - \psi(r\,,t) - D_{CJ}\,t$ is a measure of distance from the instantaneous disturbed shock position. The particle velocity we use is

$$\mathbf{u} = \mathbf{u}^l - D_{CJ}\,\mathbf{e}_z \equiv u_r\,\mathbf{e}_r + u_z\,\mathbf{e}_z \quad . \tag{2.9}$$

The fluid description is given by the equations for a reactive Euler fluid, specialized to our EOS and rate law. These equations reflect conservation of mass, momentum, energy and a rate equation for the heat release. The equations that we list have been derived from the basic set and are computationally more convenient.

The governing equations we use are:

$$\textit{mass}: N(\rho) + \mathbf{M}\cdot(\rho\mathbf{u}) = 0 \quad , \tag{2.10}$$

$$\textit{master}: \rho^{-1}N(P) - N(\tfrac{1}{2}\,\mathbf{u}\cdot\mathbf{u}) - \mathbf{u}\cdot\mathbf{M}(\tfrac{1}{2}\,\mathbf{u}\cdot\mathbf{u}) + c^2\mathbf{M}\cdot\mathbf{u} = (\gamma-1)\delta^2 qR \quad , \tag{2.11}$$

$$\textit{momentum}: N(\mathbf{u}) + \mathbf{u}\cdot\mathbf{M}(\mathbf{u}) + \rho^{-1}\mathbf{M}(P) = 0 \quad , \tag{2.12}$$

$$\textit{vorticity}: N(\rho^{-1}\omega) + \mathbf{u}\cdot\mathbf{M}(\rho^{-1}\omega) = \rho^{-1}[(\rho^{-1})_{,r}\,P_{,z} - (\rho^{-1})_{,z}\,P_{,r}]\,, \tag{2.13}$$

$$\textit{rate}: N(\lambda) + \mathbf{u}\cdot\mathbf{M}(\lambda) = R \quad , \tag{2.14}$$

with

$$R = k \;;\; 0 \leqslant \lambda < 1$$

$$R = 0\,; \quad \lambda = 1 \quad ,$$

and where k is a constant. The symbols used above are

$$\nabla \equiv \mathbf{e}_z\frac{\partial}{\partial z} + \mathbf{e}_r\frac{\partial}{\partial r} \quad , \quad \mathbf{M} \equiv \nabla - \psi_{,r}\,\mathbf{e}_r\frac{\partial}{\partial z} \quad ,$$

$$N \equiv \frac{\partial}{\partial t} - \tilde{\psi}_{,t}\,\frac{\partial}{\partial z}\ , \qquad \omega \equiv u_{r,z} - u_{z,r} + \tilde{\psi}_{,r}\,u_{z,z}\ , \tag{2.15}$$

and where $c^2 = \gamma P/\rho$ is the frozen sound speed.

The shock conditions that we write down reflect the strong shock approximation (i.e., formally setting $P_0 = 0$). Immediately behind the shock at $z = 0$, the state variables are denoted by a plus subscript. The shock conditions are

$$\rho_0/\rho_+ = \gamma(\gamma+1)^{-1} - (\gamma+1)^{-1}S\ , \tag{2.16}$$

$$u_{z_+}/D_{CJ} = -1 + (\gamma+1)^{-1}(1+S)(1+\tilde{\psi}_{,t}/D_{CJ})[1+(\tilde{\psi}_{,r})^2]^{-1}, \tag{2.17}$$

$$u_{r_+}/D_{CJ} = -(1+u_{z_+}/D_{CJ})\tilde{\psi}_{,r}\ , \tag{2.18}$$

$$P_+ = \rho_0 D_{CJ}^2(1+u_{z_+}/D_{CJ})(1+\tilde{\psi}_{,t}/D_{CJ})\ , \tag{2.19}$$

where

$$S \equiv \sqrt{1 - (1-\delta^2)[1+(\tilde{\psi}_{,r})^2]/(1+\tilde{\psi}_{,t}/D_{CJ})^2}\ . \tag{2.20}$$

Also $\lambda = 0$ at $z = 0$.

The vorticity across the shock can be calculated explicitly, see Hayes [5], as

$$\boldsymbol{\omega}_+ = -\mathbf{e}_\omega(\rho_+ - \rho_0)^2[(D_{CJ}+\tilde{\psi}_{,t})\tilde{\psi}_{,r}\,\tilde{\psi}_{,rr} - \tilde{\psi}_{,rt}]/\rho_+\rho_0[1+(\tilde{\psi}_{,r})^2]\ , \tag{2.21}$$

where $\mathbf{e}_\omega$ is the third unit vector in the 3-D orthogonal coordinate triad $\mathbf{e}_z$, $\mathbf{e}_r$, $\mathbf{e}_\omega$. In all the calculations we will refer to (i.e., to the order that we calculate) the flow can be taken to be irrotational.

3. The dynamics of the 1-D detonation

As a precursor to the solution of the full problem with the edge rarefaction, we examine the purely 1-D problem and explain its dynamics. The most important thing that we will show is that when the steady 1-D solution is perturbed, the natural time scale for the evolution of the flow is $t_1 \equiv \delta t$ or $t \sim O(\delta^{-1})$.

First we consider the steady solution. It can be represented by the expansions

$$\begin{aligned} u_z &= -D_{CJ}\alpha^{-1} + \delta D_{CJ}(\gamma+1)^{-1}u + \delta^2 u^{(2)} + \cdots , \\ P &= \rho_0 D_{CJ}^2 (\gamma+1)^{-1} + \delta P^{(1)} + \delta^2 P^{(2)} + \cdots , \\ \rho &= \alpha\rho_0 + \delta\rho^{(1)} + \delta^2\rho^{(2)} + \cdots , \quad \lambda = \lambda^{(0)} + \cdots . \end{aligned} \tag{3.1}$$

For convenience we define

$$\alpha \equiv (\gamma+1)/\gamma , \quad z^* \equiv \alpha k z / 2D_{CJ} . \tag{3.2}$$

The steady solution only depends on z^*. It is easy to show that for the assumed form of the solution, the mass, master and momentum equations lead to

$$u u_{,z^*} = 1 . \tag{3.3}$$

At leading order the rate equation is

$$\lambda^{(0)}_{,z^*} = -2 . \tag{3.4}$$

The solution of these equations must satisfy the shock boundary conditions

$$u_+ = 1 , \quad \lambda^{(0)}_+ = 0 \quad at \quad z^* = 0 . \tag{3.5}$$

These solutions have the simple form

$$u = \sqrt{1+2z^*} \ , \quad \lambda^{(0)} = -2z^* \ . \tag{3.6}$$

Note that this solution shows that to $O(\delta)$, the sonic point (i.e., where $c^2 - u_z^2$ vanishes) is precisely the location where

$$u = 0 \ , \quad \lambda^{(0)} = 1 \ , \quad z^* = -1/2 \ . \tag{3.7}$$

In addition $P^{(1)} \propto u$ and $\rho^{(1)} \propto u$.

We now show that the natural time scale for disturbances to this solution is δt. Suppose that we expand the solution as in (3.1), and we allow for dependence of the perturbed variables on both z^* and t. In addition, the shock relations indicate that we should allow for a shock velocity perturbation of the form

$$\tilde{\psi}_{,t} = \delta^2 \tilde{\psi}^{(2)}_{,t} + \cdots \ . \tag{3.8}$$

It is easy to show that u as well as $P^{(1)}$ and $\rho^{(1)}$ are only functions of z^*. However, at the next order we can show that a secularity develops in t if u is initially not identically the steady solution. Specifically we find that

$$u^{(2)} \sim t \ . \tag{3.9}$$

This difficulty is easily resolved using multiple scaling arguments in time. In particular allowing for dependence on the time scale $t_1 = \delta t$, we find that in the reaction zone u obeys the evolution equation

$$u_{,\tau} + u u_{,z^*} = 1 \ , \quad \tau \equiv \alpha k \, \delta t / 4 \ , \tag{3.10}$$

subject to the boundary condition

$$u \ \textit{prescribed at} \ z^* = -1/2 \tag{3.11}$$

and initial data on $z^* \in (-1/2, 0)$. The shock speed perturbation is given by

the shock relation

$$\tilde{\psi}_{,t} = \tfrac{1}{2}\delta^2 D_{CJ}(u_+^2 - 1) \ . \qquad (3.12)$$

Again $P^{(1)} \propto u$ and $\rho^{(1)} \propto u$. The solution of problem (3.10-11) gives a uniform description of the 1-D detonation when a disturbance is applied to the 1-D steady-state solution. Importantly the controlling time scale is t_1.

4. The dynamics of the 2-D detonation

In this section we discuss the dynamics of the 2-D detonation wave. Two features distinguish such a wave. On the scale of the reaction zone, the displacement of the leading shock from plane can be $O(1)$ or larger and the changes in the shock deflection occur over a long radial distance. Bdzil [2] has discussed the character of the steady detonation for this case and shown that the relevant radial coordinate is $r_1 \equiv \delta r$. Here we analyze the approach to the steady state for this model.

Following the steady theory, we assume that the shock locus is an $O(1)$ function that changes shape on the r_1 scale, a scale which is large compared to the reaction zone thickness. From the shock conditions, particularly (2.20), we see that time dependence will enter the $O(\delta)$ flow only if we assume a time scale $t_2 \equiv \delta^2 t$. That is, if the time scale is t_2, the quantities $(\tilde{\psi}_{,r})^2$ and $\tilde{\psi}_{,t}$ in (2.20) are of the same order. In a sense, this defines a strong interaction limit among an $O(1)$ shock locus, an $O(\delta^{-1})$ radial

variable and time. It follows that a nontrivial distinguished limit is obtained if we assume that the solution depends on the scales $\delta^2 t$ and δr. For convenience we introduce the scaled variables

$$z^* , \quad X \equiv -(\alpha^2/2)kD_{CJ}^{-1}(\delta r) ,$$
$$T \equiv (\alpha^2/4)k(\delta^2 t) . \tag{4.1}$$

Following [2] we introduce the following expansions for u_z, u_r and the shock displacement, $\tilde{\psi}$

$$u_z = -D_{CJ}\alpha^{-1} + \delta D_{CJ}(\gamma+1)^{-1}U(z^*,X,T) + \cdots ,$$
$$u_r = \delta D_{CJ}(\gamma+1)^{-1}V(z^*,X,T) + \cdots , \tag{4.2}$$
$$\tilde{\psi} = -2D_{CJ}k^{-1}\alpha^{-2}\Psi(X,T) + \cdots .$$

The expansions for P, ρ and λ are given by (3.1).

Since the flow is irrotational through $O(\delta^2)$, it follows that

$$V_{,z^*} = 0; \quad V = V(X,T) . \tag{4.3}$$

Applying the shock condition to (4.3), we find

$$V = -\Psi_{,X} . \tag{4.4}$$

The mass, master and z-component momentum equations lead to

$$UU_{,z^*} - V_{,X} = 1 . \tag{4.5}$$

Substituting (4.4) into (4.5), in the reaction zone we obtain

$$UU_{,z^*} + \Psi_{,XX} = 1 . \tag{4.6}$$

Equation (4.6) is exactly the steady-state result, so that to $O(\delta^2)$ the governing PDE's are steady. The only time dependence in the solution enters from the $O(\delta)$ shock condition

$$U_+ = \sqrt{1-\Psi_{,T}-(\Psi_{,X})^2} \quad at\ z^* = 0\ . \tag{4.7}$$

Solving (4.6) subject to (4.7), gives the solution

$$U = \sqrt{(1-\Psi_{,XX})2z^* + [1-\Psi_{,T}-(\Psi_{,X})^2]}\ . \tag{4.8}$$

The $O(\delta)$ solution, (4.8), can be thought of as a quasi-steady result.

For the unsupported detonation that we are considering, the flow must be transonic in the reaction zone. Requiring the flow to be transonic and U to be real, forces

$$U = 0 \quad at\ z^* = -\tfrac{1}{2}\ . \tag{4.9}$$

Condition (4.9) can be rigorously derived by requiring that the $O(\delta^2)$ solution be free of a secular nonuniformity in t_2. Applying this condition to (4.8) shows that the shock displacement must satisfy the evolution equation

$$\Psi_{,T} + (\Psi_{,X})^2 = \Psi_{,XX}\ . \tag{4.10}$$

Once Ψ is found, U, V, $P^{(1)}$ and $\rho^{(1)}$ are given by the simple formulas

$$U = \sqrt{1-\Psi_{,XX}}\,\sqrt{1+2z^*}\ , \quad V = -\Psi_{,X}$$
$$P^{(1)} = \rho_0 D_{CJ}^2(\gamma+1)^{-1}U\ , \quad \rho^{(1)} = \rho_0\alpha^2(\gamma+1)^{-1}U\ . \tag{4.11}$$

The solution for $\lambda^{(0)}$ is given by (3.6).

As we have shown, the dynamical character of the 1-D solution is given by the time scale t_1. In contrast, we find that for the 2-D problem the interesting dynamics occurs on a much slower time scale, specifically $t_2 \equiv \delta^2 t$. Two features of this solution are the most significant. First, this solution occupies a large spatial and temporal region of the flow and

describes a large shock deflection and flow divergence. Secondly, we find that the problem can be reduced to an evolution equation for the shock that is a second order parabolic equation in t_2 and r_1. This equation admits the steady 2-D solution which can be shown to be stable. The solution described in this section should be regarded as the principal result of this paper.

It is worth noting that if we let $\Psi_{,X} \equiv C$, one differentiation of (4.10) with respect to X yields Burgers equation for the shock slope C, namely

$$C_{,T} + 2CC_{,X} = C_{,XX} \ . \tag{4.12}$$

If we assume a different form of the rate law (i.e., other than a constant rate), then we obtain a slightly different version of (4.10) which still has parabolic character but is not Burgers equation.

We have seen that by computing Ψ, we can completely calculate the flow accurate to $O(\delta)$. The initial data for Ψ for the initial-boundary value problem that we have posed is an undisturbed flat shock, i.e.

$$\Psi = 0 \quad at \ T = 0 \quad \text{for } 0 \leqslant X < \infty \ . \tag{4.13}$$

We must specify a boundary condition at $X = 0$ to give a complete problem for Ψ. Such a boundary condition cannot be prescribed arbitrarily but must be consistent with the character of the flow near $X = 0$. A detailed discussion of the flow near $X = 0$ is given in Appendix I. There we show that the flow must be precisely sonic at $X = 0$. It then follows that the appropriate boundary condition at the vacuum interface, is

$$\Psi_{,T} + (\Psi_{,X})^2 = 1 \quad at \ X = 0 \ . \tag{4.14}$$

Thus the problem for Ψ is equation (4.10) with initial condition (4.13) and boundary condition (4.14). The steady solution is determined with the additional boundary condition that

$$\Psi(0,T) = 0 \ , \tag{4.15}$$

and given simply by

$$\Psi = -\ln(X+1) \ . \tag{4.16}$$

Equation (4.16) shows that for the semi-infinite explosive problem, the shock at the edge falls an infinite distance behind the undisturbed shock.

The linear stability of (4.16) can be investigated most conveniently by introducing the Hopf-Cole variable Φ, such that

$$\Psi = -\ln(\Phi) \ . \tag{4.17}$$

The variable Φ satisfies the ordinary heat equation and the problem in the new variable is nonlinear in the edge boundary condition placed on Φ. The perturbation of Φ about the steady state, $1+X$, satisfies a simple linear problem which can be solved exactly using a Laplace transform in time. This analysis shows linear stability to infinitesimal disturbances, where for T large

$$\Phi - (1+X) \sim -erf\,[X/(2T^{1/2})] - \frac{2T^{1/2}}{\sqrt{\pi}}\left[\frac{(X+2T)+2T}{(X+2T)^2+(2T)^2}\right]\exp[-X^2/(4T)] + \cdots \ , \tag{4.18}$$

with

$$\Phi - (1+X) \sim -\frac{1}{\sqrt{\pi} T^{1/2}} + \cdots \quad at \; X = 0 \; . \tag{4.19}$$

The solution for Ψ for small times can also be found analytically. This limiting solution exhibits some of the properties of region P that we will require later in our analysis. We find that for T small

$$\Psi \simeq 1 - \Phi = (T + X^2/2)\, erfc\,[X/(2T^{1/2})] - (1/\sqrt{\pi})\, XT^{1/2} \exp[-X^2/(4T)] + \cdots \; . \tag{4.20}$$

Also, we find U and V are

$$\begin{aligned} U &= \sqrt{1 - erfc\,[X/(2T^{1/2})]}\,\sqrt{1 + 2z^*} + \cdots \; , \\ V &= \alpha^{-1/2} 2T^{1/2} \left[(1/\sqrt{\pi}) \exp[-X^2/(4T)] - (X/2T^{1/2})\, erfc\,[X/(2T^{1/2})] \right] + \cdots \; . \end{aligned} \tag{4.21}$$

The complete solution for Ψ was found numerically. The results of these calculations are displayed in Sections 5. and 6.

5. Evolution near the wave head

In this section we point out some of the deficiencies of the solution presented in Section 4. and show how they are resolved by the existence of a purely hyperbolic region near the wave head of the original disturbance (defined here as the left-most point on the shock disturbed from the 1-D steady shock).

It should be emphasized that the existence of the wave head is a physically imposed boundary condition that is required by the hyperbolic

character of our problem. To the left of the wave head, the shock must be completely undisturbed (consistent with the initial data) since it lies outside the region of influence of the disturbance (rarefaction).

The solution of Section 4. suffers from a deficiency shown clearly by formula (4.20) for Ψ. No matter how large X is, Ψ is nonzero; there is no finite X such that Ψ is identically zero. Thus the solution fails to satisfy the physical boundary condition.

In the standard way, failure of an asymptotic solution to satisfy a globally imposed boundary condition implies the existence of an adjacent adjustment layer. Certain features of this layer are quite clear. We expect that if the adjustment region is to predict the wave head then it must be a hyperbolic region (we will hence refer to it as region H and to the parabolic region of Section 4. as region P). Examining the region-P solution we find that far into the interior of the flow the shock displacement Ψ is small, the transverse disturbances are small and the flow is nearly 1-D. Since this weakly 2-D flow must connect to the 1-D region, the results of Section 3. strongly suggest that the relevant time scale for region H is t_1.

The solution in region H must formally match with the solution in region P and this requirement puts an additional restriction on the scaling allowed in region H. In particular if the dynamics of H occur on t_1 and the dynamics of P occur on t_2, then we expect that the early-time result of P

must match with the late-time result of H. For early times the spatial dependence of region P is represented by the similarity variable (in original variables)

$$r/t^{1/2} \quad . \tag{5.1}$$

During the matching we expect that this representation of the spatial dependence is maintained between regions P and H. Indeed there is a precedent for this type of matching found in the work of Stewart [6]. There it was found, in the context of a 1-D time-dependent problem describing transition to detonation, that the short-time hyperbolic phase matched to a long-time parabolic phase via a spatial dependence represented by similarity variables. Given this principle we see that if t_1 governs the dynamics of H, then we are forced to introduce the length scale

$$r_{1/2} \equiv \delta^{1/2} r \quad , \tag{5.2}$$

in region H, if the similarity variable (5.1) is to be of $O(1)$.

5.1 Formulation of region H

With these principles in mind we now turn to the description of region H and look for a solution in terms of the scaled variables z^*, x and τ, where x and τ are defined by

$$\begin{aligned} x &\equiv -(\alpha^{3/2}/2)kD_{CJ}^{-1}(\delta^{1/2}r) = X/(\alpha\delta)^{1/2} \\ \tau &\equiv (\alpha/4)k(\delta t) = T/(\alpha\delta) \quad . \end{aligned} \tag{5.3}$$

The form that we use for the dependent variables u_r and $\tilde{\psi}$ in region H is different from the one used in region P. Equation (3.12) shows that the

shock-velocity perturbation in the 1-D time-dependent problem is $O(\delta^2)$. Since our assumed time scale is t_1, this suggests that $\tilde{\psi} = O(\delta)$ in region H. In turn, the shock condition (2.18) along with the $r_{1/2}$ distance scale suggests that $u_r = O(\delta^{3/2})$. Therefore we expand u_z, u_r and $\tilde{\psi}$ as

$$\begin{aligned} u_z &= -D_{CJ}\alpha^{-1} + \delta D_{CJ}(\gamma+1)^{-1}u(x,z^*,\tau) + \cdots , \\ u_r &= \delta^{3/2}\alpha^{1/2}D_{CJ}(\gamma+1)^{-1}v(x,z^*,\tau) + \cdots , \\ \tilde{\psi} &= -\delta\alpha^{-1}2D_{CJ}k^{-1}\psi(x,\tau) + \cdots . \end{aligned} \tag{5.4}$$

The expansions for P, ρ and λ are given by (3.1). At $O(\delta)$ the mass, energy, z-momentum and shock equations again give the simple results

$$P^{(1)} = \rho_0 D_{CJ}(\gamma+1)^{-1}u \quad , \quad \rho^{(1)} = \alpha^2\rho_0(\gamma+1)^{-1}u \quad . \tag{5.5}$$

At $O(\delta^2)$ the master equation gives

$$\begin{aligned} u_{,\tau} + uu_{,z^*} - v_{,x} &= 1 \quad \text{for } 0 \geqslant z^* > -1/2 , \\ u_{,\tau} + uu_{,z^*} - v_{,x} &= 0 \quad \text{for } z^* \leqslant -1/2 \quad , \end{aligned} \tag{5.6}$$

while the r-momentum equation at $O(\delta^{3/2})$ and the elimination of $P^{(1)}_{,x}$ using (5.5a) shows that to leading order the flow is irrotational

$$u_{,x} + v_{,z^*} = 0 \ . \tag{5.7}$$

The last two equations plus appropriate boundary conditions and initial data form a hyperbolic system for u and v. We will show that this system resolves the boundary condition difficulty in region P.

We assume that the initial data for (5.6-7) are simply the 1-D steady solution

$$u = \sqrt{1 + 2z^*}\ , \quad v = 0 \quad at\ \tau = 0\ . \tag{5.8}$$

Equation (5.8) is appropriate if and only if the 1-D region is stable to local transverse perturbations. In Section 5.2 we show that the 1-D region is stable. From the shock conditions it follows that

$$u_+ = \sqrt{1 - \psi_{,\tau}}\ , \quad v_+ = -\psi_{,x} \quad at\ z^* = 0\ . \tag{5.9}$$

The boundary conditions at the edge $x = 0$, $-\frac{1}{2} \leqslant z^* \leqslant 0$, and at the end of the reaction zone $z^* = -\frac{1}{2}$ do not follow so easily. We require that the flow be sonic on both:

$$u = 0 \quad at\ z^* = -\tfrac{1}{2} \quad \text{and} \quad on\ x = 0\ , -\tfrac{1}{2} \leqslant z^* \leqslant 0\ . \tag{5.10}$$

These last conditions are discussed in detail in Appendix II. Here we simply argue for the appropriateness of these boundary conditions. At early times in the evolution of the full problem, there is no region P just region H. Condition (5.10) is consistent with the fact that the flow at $x = 0$ is sonic at the shock for an unconfined explosive (see Appendix I) and that region H is adjacent to the 1-D flow, where $u = 0$ at $z^* = -\frac{1}{2}$. The data provided by (5.10) determine the form of the solution at the wave head for all times. As time progresses, the wave head (i.e., the furthest point of disturbance on the shock) propagates into the interior of the flow. After a sufficiently long time, the wave head is far into the explosive as measured from the edge and the solution there is not sensitive to all the details of the edge start-up transient. Then the region-H solution must be consistent with the region-P solution, which has the property that the flow is sonic at $z^* = -\frac{1}{2}$ and

$x = 0$. Since we are primarily interested in the flow near the wave head at long times when region P governs the flow near $x = 0$, (5.10) is certainly compatible with the region-P problem. Later we show that regions H and P do indeed match.

In summary, the complete problem for region H is represented by (5.6-7) solved subject to (5.9), (5.10) and the initial data (5.8). The problem is essentially a nonlinear wave propagation problem on a membrane bounded by the boundaries of the shock and the sonic locus. At time zero the equivalent of an impulse is applied to the membrane along $x = 0$, since the sonic condition imposed is inconsistent with the 1-D solution. A disturbance then propagates into the interior at a finite speed, defining the wave head as well as the complete domain of influence.

The form of the governing equations for region H could have been anticipated. Equations similar to (5.6-7) arise in other 2-D nonlinear-wave problems. Equation (5.6) with a zero right hand side and (5.7) are used to describe the unsteady flow around an oscillating transonic airfoil. Cole [7] discusses the airfoil problem and some of the properties of this hyperbolic system, including the infinite speed of the backward characteristic. Equation (5.6) with the source term on the right hand side replaced by linear dispersion and (5.7) is the weakly 2-D Korteweg-de Vries (KdV) equation. Bryant [8] used this system to describe the oblique interaction of water waves. Some of the mathematical properties of the 2-D KdV equation are

discussed by Johnson [9].

We continue the analysis of our problem by introducing a potential into (5.6-7). Making this change of variable and writing the solution as the 1-D steady-state solution plus a deviation

$$u = \zeta + \zeta^{-1}\phi_{,\zeta} \ , \quad v = -\phi_{,x} \ , \quad \zeta \equiv \sqrt{1 + 2z^*} \ , \tag{5.13}$$

in the reaction zone (5.6-7) become

$$\phi_{,\zeta\tau} + \phi_{,\zeta\zeta} + \zeta\phi_{,xx} + \tfrac{1}{2}[(\zeta^{-1}\phi_{,\zeta})^2]_{,\zeta} = 0 \ . \tag{5.14}$$

Equation (5.14) is to be solved subject to the sonic locus condition (see Appendix II)

$$\zeta^{-1}\phi_{,\zeta} = 0 \quad at \ \zeta = 0$$

$$\zeta^{-1}\phi_{,\zeta} = -\zeta \quad at \ x = 0 \ ; \quad 0 \leqslant \zeta \leqslant 1 \ , \tag{5.15}$$

the shock conditions, which can be rewritten as

$$[1 + \phi_{,\zeta}]\phi_{,\zeta x} + \tfrac{1}{2}\phi_{,x\tau} = 0 \quad at \ \zeta = 1 \ , \tag{5.16}$$

and the initial condition

$$\phi = 0 \quad at \ \tau = 0 \ . \tag{5.17}$$

It would be difficult to find the complete solution of the nonlinear problem that governs region H. However, only the long-time asymptotic solution is required of H to formally show that regions P and H match. We now turn to this question.

If we write the region P solution (4.21) in region H variables and take the limit as $\delta \to 0$, we immediately see that the spatial dependence of region P is retained through the similarity variable

$$\sigma = x/\tau^{1/2} \ . \tag{5.18}$$

The small time solution of P is the relevant one for matching with the long time solution of H and in particular (4.21) gives the matching condition that

$$u \equiv \zeta + \zeta^{-1}\phi_{,\zeta} = \zeta\sqrt{1 - erfc\,[\sigma/2]} \ , \tag{5.19}$$

$$v \equiv -\phi_{,x} = \tau^{1/2}[(2/\sqrt{\pi})\exp[-\sigma^2/4] - \sigma\, erfc\,[\sigma/2]] \ ,$$

$$as\ \tau \to \infty \ , \quad with\ \sigma\ fixed \ .$$

Now we show that the asymptotic solution required by matching, as given by (5.19), is in fact the leading order term in a long-time expansion for the governing problem of region H. Let u and v be represented by

$$u = F(\sigma,\zeta) + O(\tau^{-1/2}) \ ,$$

$$v = \tau^{1/2} G(\sigma,\zeta) + O(1) \ . \tag{5.20}$$

Equations (5.6-7) show that at leading order

$$\zeta^{-1}FF_{,\zeta} - G_{,\sigma} = 1 \ , \quad G_{,\zeta} = 0 \ ; \quad G = G(\sigma) \ . \tag{5.21}$$

The conditions at the sonic locus require

$$F(\sigma,0) = F(0,\zeta) = 0 \ . \tag{5.22}$$

In turn, the shock condition gives rise to the differential condition

$$G - \sigma G_{,\sigma} - 2[F^2(\sigma,1)]_{,\sigma} = 0 \ . \tag{5.23}$$

The solution of this problem (with the additional condition that G is bounded at $\sigma = \infty$) is straightforward and shows that

$$F = \zeta\sqrt{1 - erfc\,[\sigma/2]} \ , \tag{5.24}$$

$$G = (2/\sqrt{\pi})\exp[-\sigma^2/4] - \sigma\, erfc\,[\sigma/2] \ ,$$

which is precisely the form of the long-time solution required by the

matching condition (5.19).

The asymptotic solution that we have exhibited for region H is the one required for matching, and has a parabolic character as illustrated by its dependence on the similarity variable σ. Indeed this solution is seemingly deficient in the sense that it does not predict the existence of a wave head. We will later show that there is a wave head in region H which takes the form of a hyperbolic precursor that precedes the larger parabolic-type region moving into the 1-D detonation.

5.2 The linear stability of region H

In this section we consider the linear hydrodynamic stability of the 1-D steady-state solution. In the region of the flow that is uninfluenced by the edge rarefaction, it is important to have a stable 1-D solution so that the flow into which the rarefaction propagates is simple. It is unlikely that any analytical progress could be made on the edge-rarefaction problem if the 1-D steady solution were unstable. One reason for introducing the small resolved energy-release model (2.1) was the conjecture, based on Erpenbeck's results [4], that this model is stable. We now prove that the model is stable to 2-D disturbances. With some minor modifications, this analysis also gives us the solution to the hyperbolic-precursor problem.

The stability of the 1-D steady solution to small disturbances is governed by the linearized form of (5.14) and (5.16)

$$\phi_{,\zeta\tau} + \phi_{,\zeta\zeta} + \zeta\phi_{,xx} = 0 \ , \tag{5.25}$$

$$\phi_{,\zeta x} + \tfrac{1}{2}\phi_{,x\tau} = 0 \quad at \ \zeta = 1 \ , \tag{5.26}$$

the sonic condition

$$\phi_{,\zeta} = 0 \quad at \ \zeta = 0 \ , \tag{5.27}$$

plus some *nonzero* initial condition representing the arbitrary perturbation. Following Erpenbeck [10], we examine the stability of the shock. Equations (5.9) and (5.13) relate ϕ to the shock locus via $\psi_{,\tau} = -2(\phi_{,\zeta})_{\zeta=1}$.

We assume that the explosive is laterally infinite and Fourier decompose the solution in x

$$(\hat{\phi},\hat{\psi}) \equiv \int_{-\infty}^{\infty} e^{i\omega x} (\phi,\psi)\, dx \ , \tag{5.28}$$

and Laplace transform it in τ

$$\Omega \equiv \int_{0}^{\infty} e^{-s\tau} \hat{\phi}\, d\tau \ , \tag{5.29}$$

to get

$$s\,\Omega_{,\zeta} + \Omega_{,\zeta\zeta} + (i\omega)^2 \zeta\Omega = (\hat{\phi}_{,\zeta})_{\tau=0} \ , \tag{5.30}$$

$$\Omega_{,\zeta} + (s/2)\Omega = -\tfrac{1}{2}(\hat{\psi})_{\tau=0} \quad at \ \zeta = 1 \ , \tag{5.31}$$

and

$$\Omega_{,\zeta} = 0 \quad at \ \zeta = 0 \ , \tag{5.32}$$

where

$$\int_{0}^{\infty} e^{-s\tau} \hat{\psi}\, d\tau = -(\Omega)_{\zeta=1} \ . \tag{5.33}$$

Further introducing

$$Y \equiv [\Omega + s^{-1}(\hat{\psi})_{\tau=0}]\exp(s\zeta/2) \tag{5.34}$$

into (5.30-32), we get the inhomogeneous problem that we need to solve

$$Y_{,\zeta\zeta} - [(s/2)^2 - (i\omega)^2\zeta]Y = F(\zeta,s,\omega) \ , \tag{5.35}$$

$$F \equiv [s^{-1}(i\omega)^2\zeta(\hat{\psi})_{\tau=0} + (\hat{\phi}_{,\zeta})_{\tau=0}]\exp(s\zeta/2) \ , \tag{5.36}$$

$$Y_{,\zeta} = 0 \quad at \ \zeta = 1 \ , \tag{5.37}$$

and

$$Y_{,\zeta} - (s/2)Y = 0 \quad at \ \zeta = 0 \ , \tag{5.38}$$

with

$$\int_0^\infty e^{-s\tau}\hat{\psi}\,d\tau = s^{-1}(\hat{\psi})_{\tau=0} - (Y)_{\zeta=1}\exp(-s/2) \ . \tag{5.39}$$

The solution of (5.35-38) is constructed as an expansion in the eigenfunctions of the homogeneous problem, where the eigenfunctions and eigenvalues are Y_n and $(i\omega_n)$, respectively. A detailed solution of the homogeneous eigenvalue problem [i.e., (5.35-38) with $F(\zeta,s,\omega) = 0$] is presented in Appendix III. To construct a formal solution to (5.35-38) all we need is the orthogonality condition for the homogeneous problem

$$\int_0^1 \zeta Y_n Y_m\,d\zeta = 0 \ , \quad n \neq m \ . \tag{5.40}$$

The solution of (5.35-38) is

$$Y = \sum_{n=1}^{\infty} [(i\omega)^2 - (i\omega_n)^2]^{-1} C_n Y_n \ , \tag{5.41}$$

where

$$F(\zeta,s,\omega) = \sum_{n=1}^{\infty} C_n \zeta Y_n \quad , \tag{5.42}$$

with

$$C_n = \int_0^1 F\, Y_n\, d\zeta \Big/ \int_0^1 \zeta Y_n^2\, d\zeta \quad , \tag{5.43}$$

where from (5.39) the Laplace transform of the shock locus is

$$\int_0^{\infty} e^{-s\tau}\hat{\psi}\, d\tau = s^{-1}(\hat{\psi})_{\tau=0} \tag{5.44}$$

$$- \sum_{n=1}^{\infty} [(i\omega)^2 - (i\omega_n)^2]^{-1} C_n (Y_n)_{\zeta=1} \exp(-s/2) \quad .$$

Now the Laplace transform $C_n\ (Y_n)_{\zeta=1}$ is the Laplace transform of a bounded function of τ (i.e., the initial data) and is therefore regular throughout the domain of interest [10]. Thus the only poles of $\int_0^{\infty} e^{-s\tau}\hat{\psi}\, d\tau$ that are of interest in performing the inverse Laplace transform to get $\hat{\psi}$ are those of $[(i\omega)^2 - (i\omega_n)^2]^{-1}$. The question of stability is therefore determined by the sign of the real part of the roots, $s_n(\omega)$, of the equation

$$(i\omega)^2 - (i\omega_n)^2 = 0 \quad . \tag{5.45}$$

The limiting form of the eigenvalues for both s small and large are calculated in Appendix III

$$s - small: \quad i\omega_1 \sim s^{1/2} + \cdots \tag{5.46}$$

$$i\omega_n \sim [1/8 + 3(n-2)/2]\pi + O(s^{1/2}) \quad , \quad n = 2,\cdots$$

$$s - large: \quad i\omega_n \sim s/2 - (\alpha'_n/2)(s/2)^{1/3} + O[(s/2)^{-1/3}] \quad , \tag{5.47}$$

$$\alpha'_n \sim -[(3\pi/8)(4n-3)]^{2/3} \ . \tag{5.48}$$

Solving (5.45) for s, we get one root for $|\omega|$ small

$$s_1 \sim -|\omega|^2 + \cdots \ , \tag{5.49}$$

and for $|\omega|$ large

$$s_n \sim \pm 2|\omega| i \ + (\alpha'_n/2)|\omega|^{-2/3}(\pm i + \sqrt{3}) + \cdots \ , \quad n = 1,\cdots \ . \tag{5.50}$$

For the limits $|\omega|$ small and large, $Re(s) < 0$. Thus in these limits the 1-D steady-state solution is *stable* to small transverse disturbances.

5.3 The solution near the wave head

With this result in hand, we now construct the solution to (5.14) that satisfies the edge rarefaction boundary condition, $u = 0$ at $x = 0$ for $0 \leqslant \zeta \leqslant 1$, or equivalently

$$\phi_{,xx} = 1 \quad at \ x = 0 \ . \tag{5.51}$$

This condition forces u to deviate by an $O(1)$ amount from the steady-state solution $u = \zeta$. Thus at early times, when the wave head is near the edge, the full nonlinear problem (5.14-17) needs to be solved. At late times, (5.24) shows that the solution to (5.14-17) far from the wave head matches into the region P solution (5.19). That is at late times, the $O(1)$ deviations of u from the steady-state solution are carried by the region P solution (4.11). Therefore, we expect that the linearized form of (5.14-17) will provide an adequate representation of the flow near the wave head at late times.

It would be desirable to find the solution to the full nonlinear problem (5.14-17) for all times. However the nonlinear problem is not amenable to analysis. The best that one could do would be to find a numerical solution. What we propose to do instead is solve the linear model problem (5.25-27) subject to the conditions (5.51) and (5.17). Then we show that for long times, the solution can be represented by (5.20) provided that we are not too close to the edge (i.e., in the limit that *erfc* in (5.24) is small).

Near the wave head the solution has a much different character. It is known [11] that the high-frequency temporal components govern the behavior of the solution near the wave head. It is not clear whether the solutions of the linear and nonlinear problems are the same near the wave head at early times. The best we can say is that we've solved some boundary-value problem that has the edge boundary condition $(\phi_{,xx})_{x=0} = 1$ at long times.

Laplace transforming the velocity potential ϕ as in (5.29) and (5.34), requiring (5.17) and assuming that the x-dependence of the solution is given by $e^{-i\omega_n x}$, we construct the solution as an eigenfunction expansion

$$Y = \sum_{n=1}^{\infty} A_n e^{-i\omega_n x} Y_n \quad , \tag{5.52}$$

where $i\omega_n$ and Y_n are eigenvalues and eigenfunctions of the homogeneous form of (5.35-38) (i.e., $F = 0$ and $(\hat{\psi})_{\tau=0} = 0$). In terms of these variables the edge boundary condition (5.51) is

$$Y_{,xx} = s^{-1}\exp(s\zeta/2) \quad at \; x = 0 \; . \tag{5.53}$$

Requiring that (5.52) satisfies (5.53) determines the coefficients A_n

$$A_n = s^{-1}(i\omega_n)^{-2}\int_0^1 \zeta \exp(s\zeta/2) Y_n \, d\zeta \Big/ \int_0^1 \zeta Y_n^2 \, d\zeta \; , \tag{5.54}$$

where the integrals appearing in (5.54) are evaluated in Appendix III. The limiting form of the eigenvalues for s small and s large are given by (5.46-48). The eigenfunctions are computed in Appendix III

$$s - small: \quad Y_1 \sim (Y_1)_{\zeta=1} \sim (Y_1)_{\zeta=0} \sim Constant \; , \tag{5.55}$$

$$s - large: \quad Y_n \sim Ai[\alpha'_n + (i\omega_n)^{2/3}(1-\zeta)] \; , \quad n = 1,\cdots \; , \tag{5.56}$$

where $Ai[\;]$ is the Airy function. Using the above results in (5.29) and (5.34), with $(\hat{\psi})_{\tau=0} = 0$, and then inverting the Laplace transform gives ϕ.

The solution near the edge and wave head will be constructed separately. Near the edge, (5.24) shows that the appropriate distance and time scales are those of the parabolic problem, $\delta^{1/2}x$ and $\delta\tau$. Thus near the edge, the small s limit of the inverse transform gives the solution

$$\phi_{,x} \sim -\frac{1}{2\pi i}\int s^{-3/2}\exp(s\tau - s^{1/2}x)\, ds \tag{5.57}$$

and

$$\phi_{,\zeta} \sim -\frac{1}{4\pi i}\int s^{-1}\exp(s\tau - s^{1/2}x)\, ds \; , \tag{5.58}$$

which on using the Bateman [12] tables become

$$v = -\phi_{,x} \sim \tau^{1/2}[(2/\sqrt{\pi})\exp[-\sigma^2/4] - \sigma \, erfc[\sigma/2]] \tag{5.59}$$

and

$$u = \zeta + \zeta^{-1}\phi_{,\zeta} \sim \zeta[1 - \tfrac{1}{2}\,erfc\,[\sigma/2]] \ . \qquad (5.60)$$

Equation (5.59) is precisely the form of the long-time solution (5.19) required by the matching condition. If we are not too near the edge, $(\sigma/2) \geqslant 1$, then the linearized solution (5.60) also agrees with the nonlinear solution (5.19). Thus the long-time solution of the linearized form of (5.14-17) matches with the region P solution, provided that we're not too near the edge.

With the issue of matching behind us we go on to the most interesting part of the solution, the behavior near the wave head. The high-frequency limit (s -large) of the inverse Laplace transform of ϕ, gives

$$\psi \sim \sum_{n=1}^{\infty} (\alpha'_n)^{-1}\,\Gamma[10/3, (2\tau - x), -\alpha'_n x/2] \qquad (5.61)$$

and for $1 \geqslant (1-\zeta) > 0$

$$\phi \sim -\sum_{n=1}^{\infty} [2\sqrt{\pi}\alpha'_n Ai(\alpha'_n)(1-\zeta)^{1/4}]^{-1} \cdot \qquad (5.62)$$

$$\cdot\,\Gamma[7/2, [2\tau - x + (1-\zeta) - 2/3(1-\zeta)^{3/2}], -\alpha'_n x/2] \ ,$$

where Γ is the inverse Laplace transform

$$\Gamma(\nu,\eta,\beta) \equiv \frac{1}{2\pi i}\int \tilde{s}^{-\nu}\exp(\tilde{s}\,\eta - \tilde{s}^{1/3}\beta)\,d\tilde{s} \ . \qquad (5.63)$$

Applying the method of steepest descents [13] in the limit η small, yields

$$\Gamma(\nu,\eta,\beta) \sim -\frac{3}{2\sqrt{\pi}}(3\eta)^{\nu-1}(\beta^3/3\eta)^{(1-2\nu)/4}\exp[-2\beta^{3/2}/3(3\eta)^{1/2}] \ . \qquad (5.64)$$

This completes the development of the long-time solution near the wave head.

The most striking features of this solution are contained in the exponential dependence of (5.64). The locus of the wave head (i.e., where $\Gamma(\nu,\eta,\beta) = 0$) is given by

$$\eta = 2\tau - x + (1-\zeta) - 2/3(1-\zeta)^{3/2} = 0 \ . \qquad (5.65)$$

Because of the dependence of Γ on η, not only is ϕ zero at the wave head, but *all* its derivatives are also zero. Thus the flow is smooth at the wave head. The $\beta-$dependence of the exponential (i.e., $-\alpha'_n x/2$) shows that the signal near the wave head (i.e., $\eta = O(1)$) is strongly damped. As a result, for long times the signal near the wave head is extremely small and to first approximation is adequately represented by the first term in the series (5.61) and (5.62). Such a weak signal would be difficult to resolve both with a numerical solution and also experimentally. Specializing (5.65) to the shock and writing the result in dimensional variables, we have

$$r = -D_{CJ}(\delta/\alpha)^{1/2} t \sim -(c^2 - u_z^2)^{1/2}_{\zeta=1} t \ . \qquad (5.66)$$

This is in exact agreement with Whitham's [14] result for the speed with which an acoustic disturbance travels along a shock. Thus for the problem of the propagation of an edge rarefaction into a detonation reaction zone, we have another example of a wave-hierarchy problem where the hydrodynamically significant signal is not propagated at the wave front.

In summary, we have shown that the hyperbolic equations (5.6-7) have a 1-D steady-state solution that is stable to transverse disturbances. These equations also describe the interaction of an edge rarefaction with a

detonation reaction zone. For this problem they predict that the region of 2-D time-dependent flow is separated from the 1-D steady flow by a distinct wave head whose intersection with the shock propagates at a fixed velocity. The flow at the wave head is continuous, and at late times the 2-D signal near the wave head is very weak. Far from the wave head the shock perturbation becomes large and the flow has a diffusive character. This diffusive flow matches into the quasi-steady flow described in Section 4. In this region the large shock displacement is governed by the parabolic equation (4.10).

Figure 2 shows snapshots of the shock locus, wave head and the end of the reaction zone, expressed in terms of the variables of region P, at $T = 0.5$ and $T = 1.0$ for $\delta = 0.1$ and $\alpha = 4/3$. The composite shock locus was constructed by plotting the minimum at a given X of the set {high-frequency hyperbolic Ψ, low-frequency hyperbolic Ψ, parabolic Ψ}. A numerical solution for the parabolic region Ψ was found using the International Mathematical and Statistical Library (IMSL) software package DPDES. For $T \geq 0.5$ and the parameter values selected, only the left most 12% of the 2-D flow region is governed by the hyperbolic equations. Also the distance between the actual hydrodynamic wave head and the region where an appreciable shock deflection is observed (which might be considered as the location of the "apparent" wave head) is large.

6. Discussion of results and summary

In this section we discuss the features of our calculations that we believe are generally applicable for describing the propagation of 2-D detonation waves in condensed phase explosives.

In the context of the explosive model considered, we've shown that region P is the largest and most important region of the flow. The largest shock deflections and flow divergences are obtained in this region. Since the dynamics of the largest flow region is controlled by a relatively simple parabolic problem, it is possible to calculate experimentally important transient features of the flow in a simple way. For example, we can consider how long it takes for the 1-D wave, subjected to side rarefactions, to become a steady 2-D wave.

To answer this question we now consider a slight extension of our work which is based on the assumption that the main characteristics are controlled by the parabolic problem. We consider the initiation of a finite-width slab-geometry rate stick by a 1-D detonation. This problem is controlled by

$$\Psi_{,T} + (\Psi_{,X})^2 = \Psi_{,XX} \quad , \tag{6.1}$$

subject to the wall boundary condition

$$\Psi_{,T} + (\Psi_{,X})^2 = 1 \quad , \tag{6.2}$$

a symmetry condition on the centerline

$$\Psi_{,X} = 0 \quad at \; X = R \;, \tag{6.3}$$

where R is the scaled charge size, and the initial condition

$$\Psi = 0 \quad at \; T = 0 \;. \tag{6.4}$$

The above problem has a steady traveling wave solution, which is given by

$$\Psi = AT - \ln\cos[\sqrt{A}\,(X - R)] + Constant \;, \tag{6.5}$$

where A is the steady velocity deficit (i.e., it defines the steady-wave speed for the 2-D detonation), given by

$$D_{CJ}(1 - \delta^2 A/2) \;. \tag{6.6}$$

We can find a relationship between the velocity deficit and the charge size (similar to the steady result in [1]), as

$$R = \sqrt{A^{-1}}\tan^{-1}(\sqrt{A^{-1} - 1}) \;. \tag{6.7}$$

In the limit of a small velocity deficit, (6.7) becomes

$$R \sim (\pi/2)\sqrt{A^{-1}} - 1 + \cdots \;. \tag{6.8}$$

Equation (6.8) gives a 10% or better result for R when $A \leqslant 0.5$ and shows that $A \propto R^{-2}$ for large R.

When Ψ can be represented as (6.5) plus a small perturbation, an analytical solution of (6.1-4) is easily found. This linearized problem shows that the final approach to (6.5) goes like

$$(A - \Psi_{,T})/A \sim Constant\,[1 - 4\sin^2[\sqrt{A}\,(X - R)]]\exp(-8AT) \;, \tag{6.9}$$

where $(A - \Psi_{,T})/A$ measures the fractional departure of the local shock velocity from its 2-D steady-state value. Equation (6.9) shows that in the

final stages, the decay constant is $8A$. Combining this with (6.8), we find that when R is large, the damping goes like $\exp(-2\pi^2 R^{-2}T)$. Thus $(R^{-2}T)$ is the fundamental scaled variable for large explosive charges at long times. The trigonometric dependence in (6.9) shows that the velocity is a decreasing function of time at the center ($X = R$) and an increasing function of time at the edge ($X = 0$). At the intermediate value $X = R + \sqrt{A^{-1}}\sin^{-1}(½)$, (6.9) shows that $(A - \Psi_{,T})/A = 0$.

In order to determine the range of validity of the linearized result, numerical simulations of (6.1-4) were performed using the IMSL routine DPDES. The values of $(A - \Psi_{,T})/A$ vs. T at the center and the edge, obtained from the simulations, are plotted in Fig. 3 for the case $A = 0.1$. The results obtained with the simulations are certainly in qualitative agreement with (6.9). For the case considered in Section 5. (i.e., $\delta = 0.1$ and $\alpha = 4/3$), (5.66) predicts that the wave head reaches the center of the charge at $T \simeq 0.7$. Remarkably, the solution of the parabolic problem (6.1-4) shows that $(A - \Psi_{,T})/A$ at the center is very nearly equal to the initial 1-D value for $T \leqslant 0.7$. An analysis of the numerical solution for $T \geqslant 2$, shows that $\exp(-8AT)$ describes both the center and edge time dependence of the relaxation. Numerical simulations were done for other values of the parameter A. These simulations show that for $A = 0.01, 0.05, 0.1$ and 0.5, the function

$$(A - \Psi_{,T})/A \simeq 8\exp(-8AT) \ , \tag{6.10}$$

describes the relaxation at the edge for $T > 15$, 5, 2 and 0.7, respectively. Thus, (6.9) provides a reasonable approximation of the time dependence of the parabolic approximation to the rate stick problem.

For all the simulations done, it was observed that there was an early-time plateau for $(A - \Psi_{,T})/A$, during which the solution at the center is effectively undisturbed (see Fig. 3). These results suggest to us that the parabolic equation can be used for the shock (i.e., without the hyperbolic wave head) to provide a reasonable description for explosive charges that are wide enough to have a parabolic long-distance region.

In summary, we have shown that in the reaction zone, the complete solution to the 2-D time-dependent detonation edge rarefaction problem has a hyperbolic region, governed by

$$u_{,\tau} + uu_{,z^*} - v_{,x} = 1 \ , \tag{6.11}$$

$$u_{,x} + v_{,z^*} = 0 \ , \tag{6.12}$$

(5.8-10) and (5.15), and a parabolic region governed by

$$\Psi_{,T} + (\Psi_{,X})^2 = \Psi_{,XX} \ , \tag{6.13}$$

(4.14) and (4.15). In the limit of long time, the hyperbolic problem generates a "boundary layer" that defines the hydrodynamic wave head which makes our solution consistent with the properties of the underlying Euler equations. However in the hyperbolic region, the flow is only weakly 2-D. The bulk of the strongly 2-D flow is diffusion like and is controlled by

the parabolic equation (6.13). The practical significance of this result is that the relatively simple diffusion-like description can be used to calculate the gross shock dynamics of 2-D time-dependent detonation.

In view of these results it is interesting to speculate on two possible extensions of this work. Equation (6.13) was derived for a flow that is principally in the z^l – direction. It would be useful to derive a less coordinate dependent result, analogous to (6.13), in terms of shock centered intrinsic 2-D coordinates [15]. Such a result might have utility as a reactive "Huygens'" construction. A second more significant generalization of these results would be to extend the model to a state-dependent heat-release rate via a distinguished limit procedure. Presumably, the result of such an extension would be to replace the right hand side of (6.11) by a source term that depends on say u. This would introduce the possibility of reaction-zone instability and perhaps even Mach wave formation in the structure of the detonation reaction zone.

Acknowledgment

This work was supported by the U.S. Department of Energy (DOE-W-7405-ENG-36) and the Air Force Office of Scientific Research (AFOSR-ISSA-84-0027).

References

1. Bdzil, J.B. 1981 "Steady-state two-dimensional detonation", *J. Fluid Mech.* **108**,195-226.

2. Bdzil, J.B. 1976 "Perturbation methods applied to problems in detonation physics". In *6th Symposium on Detonation*, ACR-221, pp.352-370. U.S. GPO.

3. Fickett, W. & Davis, W.C. 1979 *Detonation*, pp. 53-54. University of California Press, Berkeley.

4. Erpenbeck, J.J. 1965 "Stability of idealized one-reaction detonations: zero activation energy". *Phys. Fluids* **8**,1192-1193.

5. Hayes, W.D. 1957 "The vorticity jump across a gasdynamic discontinuity". *J. Fluid Mech.* **2**,595-600.

6. Stewart, D.S. 1985 "Transition to detonation in a model problem". *J. Mec. Theor. Appl.* **4**,103-137.

7. Cole, J.D. 1977 "Modern developments in transonic flow". In *Proceedings of the International Symposium on Modern Developments in Fluid Mechanics* pp. 189-213. SIAM, Philadelphia.

8. Bryant, P.J. 1982 "Two-dimensional periodic permanent waves in shallow water". *J. Fluid Mech.* **115**,525-532.

9. Johnson, R.S. 1980 "Water waves and Korteweg-de Vries equations". *J. Fluid Mech.* **97**,701-719.

10. Erpenbeck, J.J. 1962 "Stability of steady-state equilibrium detonations". *Phys. Fluids* **5**,604-614.

11. Whitham, G.B. 1974 *Linear* and *Nonlinear Waves*, pp. 343. Wiley.

12. Bateman, H. 1954 *Tables of Integral Transforms — Vol. I*, pp. 245-246. McGraw-Hill.

13. Drazin, P.G. & Reid, W.H. 1981 *Hydrodynamic Stability*, pp. 466-469. Cambridge.

14. Whitham, G.B. 1974 *Linear* and *Nonlinear Waves*, pp. 294. Wiley.

15. Serrin, J. 1959 "Mathematical principles of classical fluid mechanics". In *Encyclopedia of Physics – Vol. VIII* /1, pp. 156. Springer-Verlag.

Figure captions

Figure 1 - A schematic representation of the shock locus and the end of the reaction zone ($\lambda = 1$) for a two-dimensional detonation in a small resolved heat release explosive ($\delta << 1$). The material to the right(left) of the z^1-axis is vacuum(explosive). The flow to the left of the dashed line is one dimensional (1-D), that between the dashed and chain-dot line is two-dimensional hyperbolic (H) and that to the right of the chain-dot line is two-dimensional parabolic (P).

Figure 2 - Snapshots of the two-dimensional time-dependent reaction zone at $T = 0.5$ and $T = 1.0$ for $\delta = 0.1$ and $\alpha = 4/3$. The upper part of each curve is the composite shock locus, the left part is the wave head and the lower curve is the end of the reaction zone. The one-dimensional region is denoted by (1-D), the hyperbolic region by (H) and the parabolic region by (P). The chain-dot line connects the transition points between regions P and H.

Figure 3 - Results of the numerical solution of (6.1-4) for the case $A = 0.1$. The early-time plateau exhibited by the solution at the center line is in qualitative agreement with the result that is expected from the full hyperbolic-parabolic description of the problem.

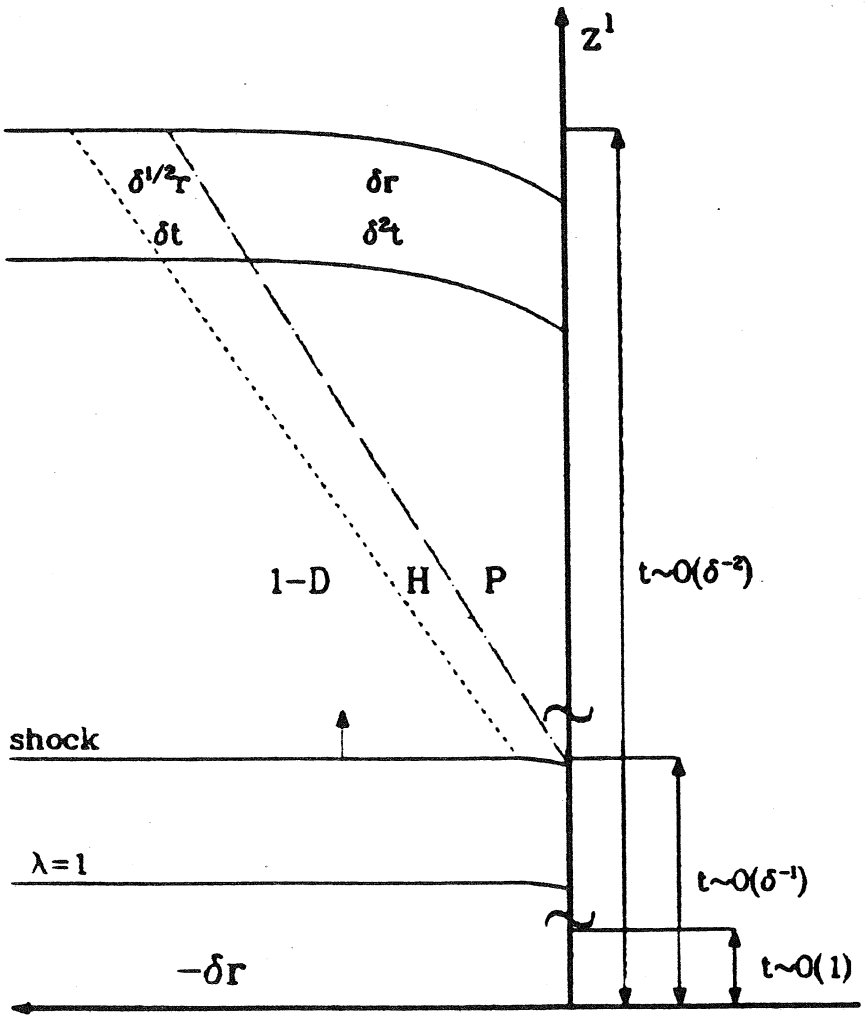

Figure 1.

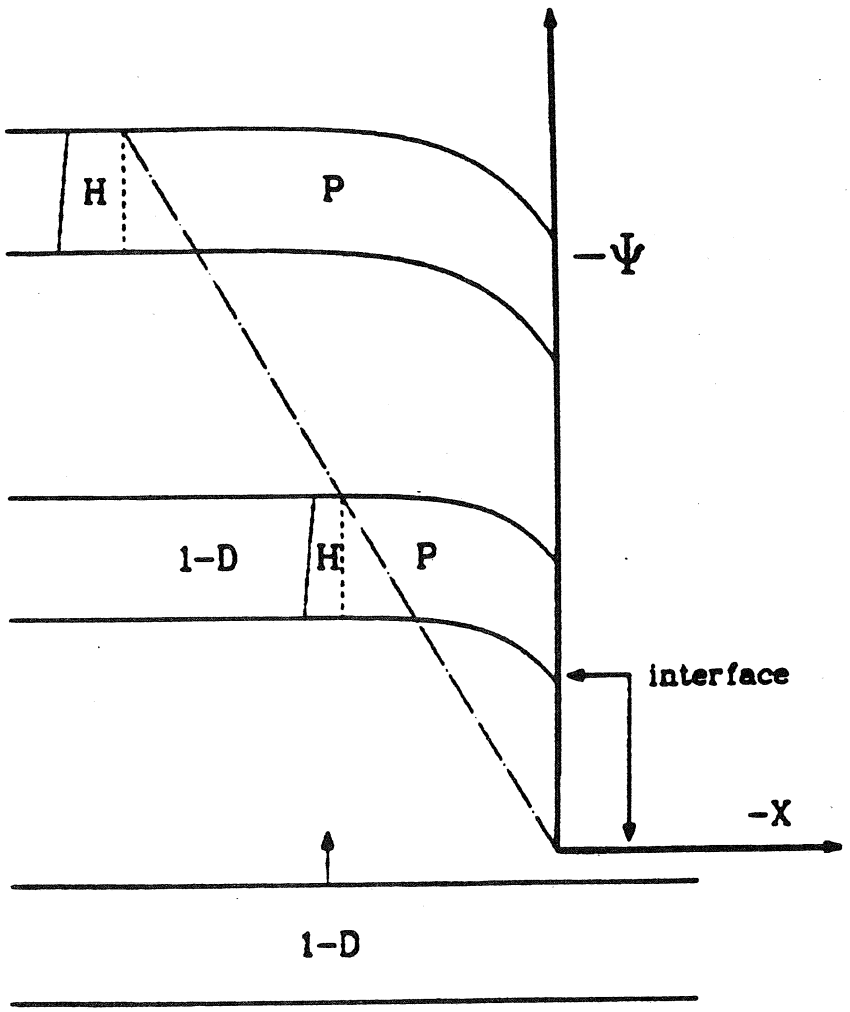

Figure 2.

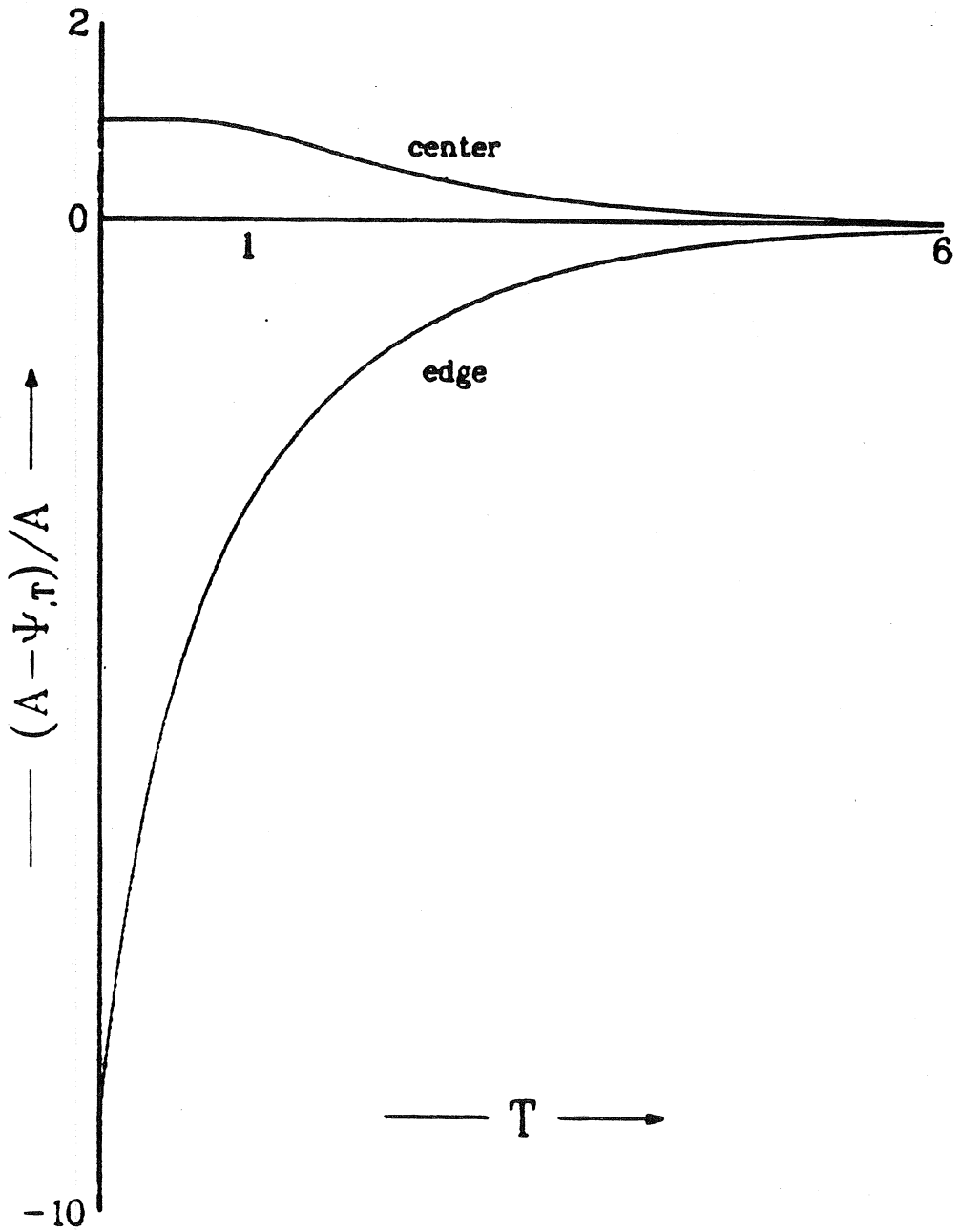

Figure 3.

Appendix I.

In this appendix we analyze the flow near the shock attachment point, which is defined as the intersection of the leading shock and the explosive-vacuum interface. The end result of the analysis derives the boundary condition (4.14).

The analysis is most easily carried out in local polar coordinates (R,θ) in a frame with its origin at the attachment point. The local polar coordinates are defined in terms of the lab coordinates z^l, r by

$$r = R\sin\theta \ , \quad z^l = R\cos\theta + \psi(0,t) + D_{CJ}t \ . \tag{A1.1}$$

The relative particle velocity, denoted by $\mathbf{u}$, is related to the particle velocity in the lab frame, $\mathbf{u}^l$, by the definitions

$$\begin{aligned} \mathbf{u} &= \mathbf{u}^l - [D_{CJ} + \psi(0,t)]\mathbf{e}_z \qquad (A1.2)\\ &\equiv u_z\,\mathbf{e}_z + u_r\,\mathbf{e}_r \equiv M\,\mathbf{e}_\theta + N\,\mathbf{e}_R \ , \end{aligned}$$

where

$$\mathbf{e}_R = \cos\theta\,\mathbf{e}_r + \sin\theta\,\mathbf{e}_z \ , \quad \mathbf{e}_\theta = \cos\theta\,\mathbf{e}_z - \sin\theta\,\mathbf{e}_r \ . \tag{A1.3}$$

In order to formulate the problem in the corner, we must rewrite the governing equations (2.10-14) and the shock conditions (2.16-19) in the new coordinates. These steps have been left to the reader.

We now show that a local solution can be constructed near the attachment point as a local coordinate expansion in R. Thus we expand the solution as

$$P = P^{(0)}(\theta,t) + O(R) , \quad \rho = \rho^{(0)}(\theta,t) + O(R) ,$$
$$u_\theta = M^{(0)}(\theta,t) + O(R) , \quad u_R = N^{(0)}(\theta,t) + O(R) ,$$
$$c^2 = (C^{(0)})^2 + O(R) \quad \text{and} \tag{A1.4}$$
$$\Psi = \Xi^{(0)}(t) + R\cos\theta\,\Xi^{(1)}(t) + O(R^2) .$$

(Note that to reduce the notation, all expansion variables and superscripts refer to the form of the R coordinate expansion in the corner.)

We expect that at leading order, the solution contains the classic Prandtl-Meyer (P-M) singularity. The expansions are introduced into the governing equations and shock conditions. After some manipulation, we find that

$$[(C^{(0)})^2 - (M^{(0)})^2][M^{(0)}_{,\theta} + N^{(0)}] = 0 , \tag{A1.5}$$
$$M^{(0)}[N^{(0)}_{,\theta} - M^{(0)}] = 0 , \tag{A1.6}$$

and

$$[(C^{(0)})^2 - (M^{(0)})^2]C^{(0)}_{,\theta} = 0 . \tag{A1.7}$$

Equations (A1.4-6) admit two special solutions, corresponding to constant state regions and a P-M fan. In fact, the entire flow near the corner is constructed from these solutions. It consists of a constant state (region 1) immediately behind the shock, followed by the P-M fan connected to another constant state (region 2) whose far boundary forms the vacuum-explosive interface (see Figure A1). The constant state immediately behind the shock is the shocked state to leading order. This requires that u_z, u_r and c^2 take on their shock values. Note that $M^{(0)}$ and $N^{(0)}$ change in region

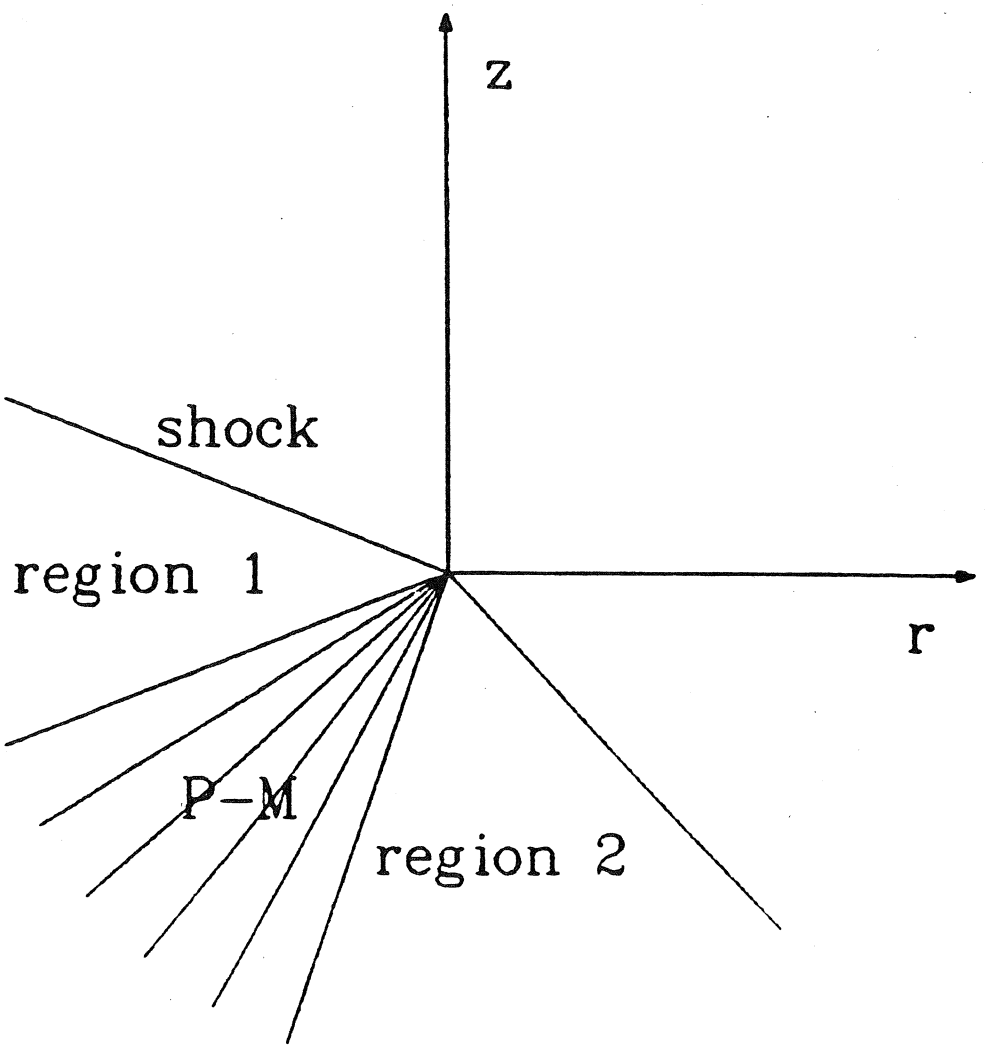

Figure A1.

1 according to the definition (A1.2).

In particular, the constant state in region 1 must then match with a state that can be attained by the P-M fan. The structure of the P-M fan is described by the condition

$$(C^{(0)})^2 - (M^{(0)})^2 = 0 \quad \text{and} \quad N^{(0)}_{,\theta} - M^{(0)} = 0 \ . \qquad \text{(A1.8)}$$

For the present purposes, it is sufficient to say that explicit values for the constant states in region 1 and 2 and a complete description of the solution in the P-M fan can be obtained.

The required boundary conditions on the shock slope can be derived in a simple way from matching the constant state behind the leading shock with the P-M fan. First we note that in the P-M fan the state is either sonic or supersonic, since

$$(C^{(0)})^2 - [(M^{(0)})^2 + (N^{(0)})^2] = -(N^{(0)})^2 \leqslant 0 \ , \qquad \text{(A1.9)}$$

whereas in region 1 we have the result that

$$(C^{(0)})^2 - [(M^{(0)})^2 + (N^{(0)})^2] \geqslant 0 \ , \qquad \text{(A1.10)}$$

for $(\Xi^{(1)})^2$ sufficiently small. Thus in order to match these regions, we must require that to leading order the flow is sonic immediately behind the shock. Thus we arrive at the condition (by making the left hand side of (A1.10) vanish identically)

$$[1 + (\Xi^{(1)})^2] = \gamma[2(\gamma+1) - (\gamma+2)E]/[(\gamma+1) - E]^2 \ , \qquad \text{(A1.11)}$$

where

$$E = D_{CJ}^2(1-\delta^2)/[D_{CJ} + \Xi_{,t}^{(0)}] \ .$$

Writing the above result in terms of region P variables and expanding for small δ, ultimately yields the result (4.14). This is a relationship between the shock velocity and the shock slope at the explosive-vacuum interface.

Appendix II.

In this appendix we formulate the boundary conditions that we apply to (5.14) at the end of the reaction zone ($\zeta = 0$) and at the edge ($x = 0$). We begin by considering the boundary $\zeta = 0$.

Since we are considering a detonation that is unsupported to the rear (i.e., for $\zeta << 0$), the boundary condition at $\zeta = 0$ will be determined locally and is not a function of the details of the inert supersonic flow near the piston ($z^l = 0$ at the piston). Rewriting (5.6) in terms of the independent variable ζ

$$(\tfrac{1}{2}u^2)_{,\zeta} = \zeta(1 + v_{,x} - u_{,\tau}) \ ; \quad \zeta > 0$$

$$(\tfrac{1}{2}u^2)_{,\zeta} = \zeta(v_{,x} - u_{,\tau}) \ ; \quad \zeta < 0 \ , \qquad \text{(A2.1)}$$

it then follows that $(\tfrac{1}{2}u^2)_{,\zeta} = 0$ at $\zeta = 0$ if $v_{,x}$ is regular. Thus either $(u)_{\zeta=0} = 0$ or $(u_{,\zeta})_{\zeta=0} = 0$. Differentiating (A2.1) with respect to ζ, yields

$$(u_{,\zeta})^2 + uu_{,\zeta\zeta} = (1 + v_{,x} - u_{,\tau}) - \zeta(\zeta u_{,xx} + u_{,\zeta\tau}) \ ; \quad \zeta > 0$$

$$(u_{,\zeta})^2 + uu_{,\zeta\zeta} = (v_{,x} - u_{,\tau}) - \zeta(\zeta u_{,xx} + u_{,\zeta\tau}) \ ; \quad \zeta < 0 \ . \qquad \text{(A2.2)}$$

The flow is initially 1-D. Therefore at $\tau = 0$, $(u)_{\zeta=0} = 0$ and $u_{,\zeta}$

experiences a jump, given by (A2.2), in response to the discontinuity in the rate. It can be shown that the ray paths for (A2.1) are purely longitudinal at $\zeta = 0$. Therefore $\zeta = 0$ is a characteristic surface and the jump in $u_{,\zeta}$ is maintained at $\zeta = 0$. From (A2.1) it follows that $(u)_{\zeta=0} = 0$ for all times, with

$$\phi = A(x,\tau) + B(x,\tau)\zeta^3 + \cdots \qquad \text{(A2.3)}$$

near $\zeta = 0$.

A more physically based argument can be made. Region H connects the 1-D undisturbed region to region P. Since the flow is sonic at $\zeta = 0$ in both of these regions [1-D, $u = \zeta$ and 2-D, $u = (1 - \Psi_{,XX})\zeta$], uniformity of the solution argues for $u = 0$ at $\zeta = 0$ in the hyperbolic region.

The form of the boundary condition at $\zeta = 0$ depends on the form of the rate law. For example, if the rate is given by $R = k(1-\lambda)$, the sonic locus is *not* everywhere coincident with the end of the reaction zone.

A rigorous boundary condition at the edge ($x = 0$) will not be derived. To do so would require a detailed analysis of the flow near the edge on distance and time scales shorter than $x = O(1)$ and $\tau = O(1)$. Instead we simply assume that $u = 0$ at $x = 0$. This is consistent with the shock result derived in Appendix I. and the $\zeta = 0$ boundary condition derived earlier in this appendix.

Appendix III.

In this appendix we determine the solution of the linear boundary-value problem

$$Y_{n,\zeta\zeta} - [(s/2)^2 - (i\omega_n)^2 \zeta] Y_n = 0 \qquad \text{(A3.1)}$$

and

$$Y_{n,\zeta} = 0 \quad at\ \zeta = 1\,, \qquad Y_{n,\zeta} - (s/2) Y_n = 0 \quad at\ \zeta = 0\,, \qquad \text{(A3.2)}$$

which on introducing the independent variable

$$\xi \equiv e^{i2\pi/3} (i\omega_n)^{-4/3} [(s/2)^2 - (i\omega_n)^2 \zeta]\,, \qquad \text{(A3.3)}$$

becomes

$$Y_{n,\xi\xi} - \xi Y_n = 0 \qquad \text{(A3.4)}$$

and

$$Y_{n,\xi} = 0 \quad at\ \zeta = 1\,, \qquad Y_{n,\xi} - \xi^{1/2} Y_n = 0 \quad at\ \zeta = 0\,. \qquad \text{(A3.5)}$$

Equation (A3.4) is the Airy equation. Its general solution can be written as a linear combination of the Airy functions $Ai(\xi)$ and $Ai(e^{-i2\pi/3}\xi)$. Forcing the solution of (A3.4) to satisfy the boundary condition at $\zeta = 1$, gives

$$Y_n = Ai(e^{-i2\pi/3}\xi) - [e^{-i2\pi/3} Ai'(e^{-i2\pi/3}\xi_{\zeta=1})/Ai'(\xi_{\zeta=1})] Ai(\xi)\,. \qquad \text{(A3.5)}$$

Requiring that (A3.5) satisfy the boundary condition at $\zeta = 1$, we get the determining equation for the eigenvalues $i\omega_n$

$$[-\xi_{\zeta=0}^{1/2} Ai(\xi_{\zeta=0}) + Ai'(\xi_{\zeta=0})] Ai'(e^{-i2\pi/3}\xi_{\zeta=1}) \qquad \text{(A3.6)}$$

$$- [-e^{i2\pi/3}\xi_{\zeta=0}^{1/2} Ai(e^{-i2\pi/3}\xi_{\zeta=0}) + Ai'(e^{-i2\pi/3}\xi_{\zeta=0})] Ai'(\xi_{\zeta=1}) = 0 .$$

The solutions of (A3.6) in the limits s -small and s -large can easily be found. When $s = 0$, (A3.6) degenerates to

$$Ai'[-(i\omega_n)^{2/3}] - Ai'[-e^{i2\pi/3}(i\omega_n)^{2/3}] = 0 , \qquad (A3.7)$$

which has the solutions

$$i\omega_1^{(0)} = 0 , \quad i\omega_n^{(0)} \sim [1/8 + 3(n-2)/2]\pi , n = 2,\cdots . \qquad (A3.8)$$

Expanding (A3.6) about (A3.7) for s -small and using the definition of the Wronskian, we find

$$i\omega_1 \sim s^{1/2} + \cdots , \qquad (A3.9)$$

$$i\omega_n \sim [1/8 + 3(n-2)/2]\pi + O(s^{1/2}) , \quad n = 2,\cdots .$$

Substituting (A3.9) into (A3.5) gives us the eigenfunctions in the s -small limit, with

$$Y_1 \sim [1 - e^{-i2\pi/3}]Ai(0) + \cdots . \qquad (A3.10)$$

The s -large limit of (A3.6) is obtained by noting that for the wave problem that we're considering, $s \propto i\omega$ and at leading order ω is real. It then follows that $\pi > arg(\xi_{\zeta=0}) > \pi/2$, so that $[-\xi_{\zeta=0}^{1/2} Ai(\xi_{\zeta=0}) + Ai'(\xi_{\zeta=0})]$ is exponentially large and $[-e^{i2\pi/3}\xi_{\zeta=0}^{1/2} Ai(e^{-i2\pi/3}\xi_{\zeta=0}) + Ai'(e^{-i2\pi/3}\xi_{\zeta=0})]$ is exponentially small. Therefore at leading order (A3.6) becomes

$$Ai'(e^{-i2\pi/3}\xi_{\zeta=1}) \sim 0 , \qquad (A3.11)$$

where the zeros of (A3.11) are

$$\alpha'_n \sim -[(3\pi/8)(4n-3)]^{2/3} , \quad n = 1,\cdots , \qquad (A3.12)$$

which yields the s -large limit of the eigenvalues

$$i\omega_n \sim s/2 - (\alpha'_n/2)(s/2)^{1/3} + O[(s/2)^{-1/3}] \ . \qquad \textbf{(A3.13)}$$

In this limit the eigenfunctions are

$$Y_n \sim Ai(e^{-i2\pi/3}\xi) \ . \qquad \text{(A3.14)}$$

The orthogonality condition for the eigenfunctions is obtained by studying

$$L \equiv Y_{n,\xi}[Y_{m,\xi} - (s/2)Y_m] - Y_{m,\xi}[Y_{n,\xi} - (s/2)Y_n] \ . \qquad \text{(A3.15)}$$

Differentiating (A3.15) with respect to ζ and then using (A3.1), we find

$$L_{,\zeta} = (s/2)[(i\omega_n)^2 - (i\omega_m)^2]\zeta Y_n Y_m \ . \qquad \text{(A3.16)}$$

Since $L = 0$ at $\zeta = 0,1$, it follows that

$$\int_0^1 \zeta Y_n Y_m \, d\zeta = 0 \ , \quad n \neq m \ . \qquad \text{(A3.17)}$$

The normality condition is obtained by studying $\int_0^1 Y_n Y_{n,\zeta\zeta} d\zeta$,

$\int_0^1 Y_{n,\zeta} Y_{n,\zeta\zeta} d\zeta$ and $\int_0^1 \zeta Y_{n,\zeta} Y_{n,\zeta\zeta} d\zeta$. Using (A3.1) and then integrating by parts, we find

$$3(i\omega_n)^2 \int_0^1 \zeta Y_n^2 d\zeta = \qquad \text{(A3.18)}$$

$$(i\omega_n)^{-2}[(i\omega_n)^2 + 2(s/2)^2][(i\omega_n)^2 - (s/2)^2](Y_n^2)_{\zeta=1} + (s/2)(Y_n^2)_{\zeta=0} \ .$$

The eigenfunctions expansion of (5.52) requires us to evaluate

$\int_0^1 \zeta \exp(s\zeta/2) Y_n \, d\zeta$. Starting with $\int_0^1 \exp(s\zeta/2) Y_{n,\zeta\zeta} d\zeta$, using (A3.1) and integrating by parts, we get

$$(i\,\omega_n)^2 \int_0^1 \zeta \exp(s\,\zeta/2) Y_n \, d\,\zeta \;=\; (s/2)\exp(s/2)(Y_n)_{\zeta=1} \;. \quad \text{(A3.19)}$$